International Journal of Recent Technology and Engineering (IJRTE)
ISSN: 2277-3878, Volume-8 Issue-3, September 2019

An Efficient Gastrointestinal Hemorrhage Detection and Diagnosis Model for Wireless Capsule Endoscopy

R. Ponnusamy, S. Sathiamoorthy

Abstract*:*Wireless Capsule Endoscopy (WCE) captures the section of human gastrointestinal (GI) tract which is impossible by the classical endoscopy investigations. A main limitation exist in the method is the requirement of analyzing massive data quantity for detecting the diseases which consumes more time and increases the burden to the physicians. As a result, there is a requirement to effectively develop an automated model to detect and diagnosis diseases on the WCEimages. The design of the presented model depends upon the examination of the patterns exist in frequency spectra of the WCE frames because of the occurrence of bleeding regions. For the exploration of the discriminating patterns,this study presents a new feature extraction based classification model is developed. An efficient Normalized Gray Level Co-occurrence Matrix (NGLCM) is applied for extracting the features of the GI images. Then, a kernel support vector machine (KSVM) with particle swarm optimization (PSO) is applied for the classification of the processed GI images. The experimentation takes place on the benchmark GI images to verify the superior nature of the presented model. The results confirmed the enhanced classifier outcome of the presented model on all the applied images under several aspects.

Keywords*: *WCE, Feature extraction, Diagnosis, Classification

I. INTRODUCTION

Traditional endoscopy process allows the physicians to examine the gastrointestinal (GI) tract of humans. In spite of being effective for the upper as well as lower portions of the GI tract, the conventional endoscopic imagesunhappily failed to investigate the small intestinewhich is 8m long. For resolving the difficulties exist in the classical endoscopy, [1] developed a new trend of wireless capsule endoscopy (WCE) which is usually a pillshape capsule. It has an inbuilt video camera, wireless transmitter, power source and a light-emitting diode and abattery. The person who needs the examination will swallow the capsule and it reaches the peristalsis of human GI tract. Then, the images will be saved since it shifts towards the GI tract and transmit it by the use of radio frequencies. It will transmit the data for a period of 8 hours till the power source get exhausted. The process involved in the WCE based medical examination is shown in Fig. 1. Because of its significant results of attaining virtual picture of GI tract, U.S. Food and Drug Administration (FDA) standardized it [2].

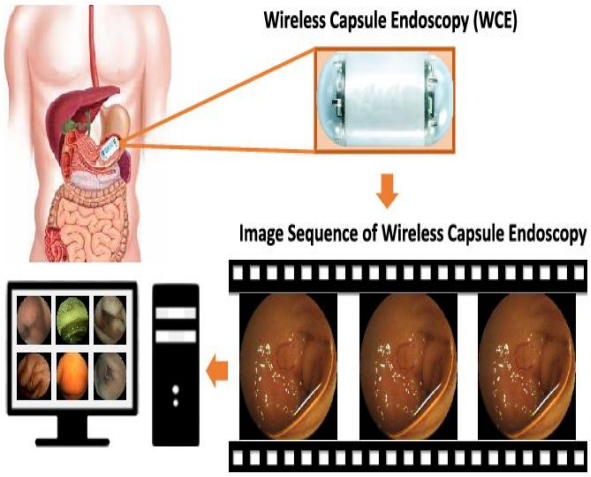

Fig. 1. Process involved in the WCE based medical examination

The process of classifying the bleeding as well as non-bleeding images from WCE images faces several difficulties. The battery power of the results restricts the outcome in lower resolution of the captured frames. At the same time, it offers slow frame rate of 2frames/s. In addition, around 6k images have to be investigated for every examination. It makes the physician to spend almost 120minutes to examine the image which is not acceptable in practical cases. As the validation procedure consumes more time, the identification of bleeding is highly prone to human error. Hence, an automated detection model for the bleeding frames could construct this massive task simple for physicians. [3] developed a program named Suspected Blood Indicator (SBI) to automatically detect the bleeding frames. However, SBIexhibits low sensitivity and specificity and frequently failed to identify various kinds of bleeding apart from small intestine.

The program developed by Given Imaging Ltd. enables the doctor to see a pair of successive frames concurrently. However, because of lower frame rate, a pair of successive frames might not have the interested region. As a result, the physician has to snap among the images to make the validation procedure highly burden and time consuming. However,

Manuscript published on 30 September 2019
* Correspondence Author
R. Ponnusamy*, Department of Computer and Information Science, Annamalai University, India. Email: povi2006@gmail.com
S.Sathiyamoorthy, Tamil Virtual Academy, India, Email ks_sathia@yahoo.com

the automated detection models can easily overcome all the above-mentioned drawbacks. Earlier studies made on GI hemorrhage identification which has been divided into color and texture, color, and both color with texture-based models. The formermodel [4] mainly makes use of the ratio of the intensity values present in RGB or HSI field. The lattermodel aims to use the textural information of the bleeding and non-bleeding images for classifying it [5]. It is observed that the integration of color as well as texture descriptors offers better results with respect to accuracy. Another time, based on the portion of operation, the detection models can be divided into whole image, pixel and patch -based models.

The models from first type are seemed to be faster, however, it fails to identify smaller bleeding portions. Pixel based model operates on every pixel present in the image for generating the feature vectors. Consequently, it has high computation complexity. The third patch-based model offers higher sensitivity by sacrificing the specificity and accuracy. In addition, informative patch requires to be detected in a manual way through a physician that hinders the concept of generating the entire process in the automated way. [6] developed a chrominance moment and Uniform Local Binary Pattern (ULBP) model to detect the bleeding. [4] devised a super-pixel and red ratio-based solution which shows optimal performance. However, it is observed that maximum computation cost and it failed to identify the images with low illumination and slight angiodysplasia region.

Few earlier studies [7, 8] make use of MPEG-7 based visual descriptor for the identification of medical events. [9] developed a 6-D feature vector employed probabilistic neural network (PNN) as a classification model. [10] projected Raw, Ratio and Histogram feature vectors that is fundamentally the intensity values of the pixels and employed support vector machine (SVM) for the detection of the GI bleeding images. [11] make use of scale invariant wavelet-based texture features for the detection of the Celiac disease in endoscopic videos. By the use of MPEG-7 based visual descriptor, Bayesian and SVM, [12] undergoes the segmentation of the GI tract into a set of four main topographical regions and carries out the categorization of the images.

From the above studies, it is revealed that there is a requirement to effectively develop an automated model to detect and diagnosis diseases on the WCE images. The design of the presented model depends upon the examination of the patterns exist in the frequency spectra of the WCE frames because of the occurrence of bleeding regions. For the exploration of the discriminating patterns, this study presents a new feature extraction-based classification model is developed. An efficient Normalized Gray Level Co-occurrence Matrix (NGLCM) is applied for extracting the features of the GI images. Then, a kernel support vector machine (KSVM) with particle swarm optimization (PSO) is applied for theclassification of the processed GI images. The experimentation takes place on the benchmark GI images to verify the superior nature of the presented model. The results confirmed the enhanced classifier outcome of the presented model on all the applied images under several aspects.

The remaining portions are planned here. Section 2 discusses the projected method in detail. Section 3 evaluates the presented approach and Section 4 provides the conclusion.

II. PROPOSED METHOD

The working process of the presented model is illustrated in Fig. 2. The figure states that the presented model involves a set of sub-processes as explained below. The input GI images undergo initial processing to remove the unwanted portions in the image. Then, the processed image undergoes feature extraction process which filters out the essential features present in the image. Consequently, the parameter tuning of SVM takes place using the PSO algorithm which will be helpful to classify theGI images into bleeding and non-bleeding regions.

A. Preprocessing

The preprocessing level comprises a set of sub processes to improve the image quality and lessen the speckles with no elimination of needed features for the identification purposes. A better option to remove the noise present in the image is to apply various filters exist in the image. In this case, median filter is employed to preprocess the GI images. When the preprocessing stage gets completed, the produced image is provided as input to the next stage.

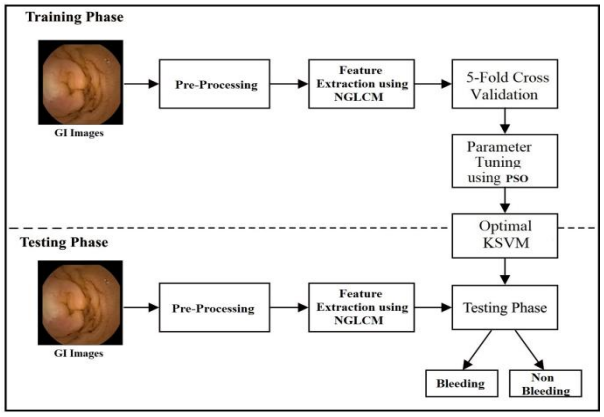

Fig. 2. Working process of proposed method

B. Feature extraction process using NGLCM

GFor capturing the local textural details from the image spectra, a set of diverse features takes place from NGLCM of magnitude spectra of the WCE frames.

GLCM is an L*L matrix of the input image where L presents the grayscale count present in the images.Fig. 3 shows the generation of the GLCM from an image. When a pair of successive pixels present in the input image having a set of pixels named m and n, then the (m, n) element gets incremented.The function takes place for each pixel pair presents in the image. By following this, GLCM is constructed. The position operator P will govern the way how the pixels are interrelated to one another. Here, the results of the NGLCM on the frequency spectra of WCE images undergo examination.

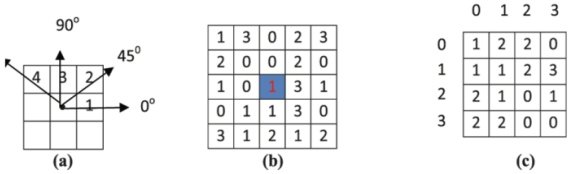

Fig.3.Generation of GLCM

The construction of the NGLCM takes place using Eq. (1):

$$N(m,n) = \frac{G(m,n)}{R} \quad (1)$$

where R represents the pixel pair count present in the GLCM. In core, NGLCM performs mapping of the images to a matrix indicating the possibility of the existence of the two successive pixel values. It indicates that NGLCM holds the local textural details of the image to be filtered using the images. In addition, the NGLCM based texture features are commonly employed in diverse applications to analyze the texture and classify the images. These two characteristics inspired the usage of the NGLCM in the presented model.
Diverse statistical metrics like mean, moment, entropy, and so on are employed as the global texture descriptors for validating the whole textural description of the image. These characteristics functions on the whole image. Once several experiments are conducted, it is identified that the entropy of the frequency spectra implies effective results. The entropy of the frequency spectra(E_{fs}) can be represented as follows:

$$E_{fs} = -\sum_{m=0}^{L-1} H(z_m) \log_2[H(z_m)] \quad (2)$$

where $H(z_m)$ represents the normalized histogram, L indicates the gray level count present in the frequency spectrum. The arbitrariness of the pixel value present in the magnitude spectrum is computed.

A set of 14 features is carried out the GLCM based texture examination. Though every feature is not commonly employed, it is investigated and determined that the below mentioned features offer better results. They are:

- Contrast(C): It computes the contrast level present in the grayscale in the nearby pixels. The value of C ranges between 0 to $(L-1)^2$.

$$C = \sum_m \sum_n |m-n|^2 N(m,n) \quad (3)$$

- Sum Entropy(S_E):

$$S_E = \sum_{m=2}^{2L} p_{x+y}(m) \log[P_{x+y}(m)] \quad (4)$$

- Sum Variance (S_V): It determines the variability of the components of NGLCM based on SE.

$$S_V = \sum_{m=2}^{2L} (m - S_V)^2 P_{x+y}(m) \quad (5)$$

- Difference Variance (D_V):
DV= Variance $[P_{x-y}]$, $where\ P_{x+y}$ and P_{x-y} is represented in Eq. (6) and Eq. (7):

$$P_{x+y}(k) = \sum_{m=1}^{L} \sum_{n=1}^{L} N(m,n) \quad m+n = k = 2,3,4,\dots,2L \quad (6)$$

$$P_{x-y}(k) = \sum_{m=1}^{L} \sum_{n=1}^{L} N(m,n) \quad |m-n| = k = 1,2,\dots,L-1 \quad (7)$$

In this study, an efficient local textural feature known as Difference Average (DA) that performs on NGLCM is presented and is defined in Eq. (8):

$$DA = \sum_{i=0}^{L-1} i P_{x-y}(i) \quad (8)$$

It is obvious that DA is the mean of $P_{x-y}(i)$. It indicates the average pixel values variations in the whole NGLCM assuming that the pixel variation has an arbitrary parameter. It is imagined that the feature offers a concept regarding the anticipated pixel variation value of NGLCM. The details are important in the circumstance of texture categorization and the usage in automated diagnosis tool. The simulation outcome exhibited that presented featuresshows discerning values from bleeding to non-bleeding frames. Here, DA is applied for classifying the textures and another identical application where remaining GLCM based features takes place.

C. PSO-KSVM based classification

Linear SVMs has the restriction on linear hyperplane that could not separate complex distributed realistic data. For the generalization in nonlinear hyperplane, the kernel trick is employed to the SVM. The resultant technique is generally same, rather than the replacement of each dot product using a nonlinear kernel function. At the same time, KSVM enables fitting of the maximum-margin hyperplane in a converted feature space. The alteration might be not linear, and the converted space has high dimension. For every kernel, a minimum of one modification variable should be present for making the kernel adaptable and tailor to the real data. Here, RBF kernel is selected because of its effective results. Then, the kernel can be defined as follows.

$$k(x_m, x_n) = \exp\left(-\frac{||x_m - x_n||}{2\sigma^2}\right) \quad (9)$$

The concluding SVM training function is defined by

$$\max_{\alpha} \sum_{n=1}^{N} \alpha_n - \frac{1}{2} \sum_{n=1}^{N} \sum_{m=1}^{N} \alpha_m \alpha_n y_m y_n \exp\left(-\frac{||x_m - x_n||}{2\sigma^2}\right) \quad (10)$$
$$s.t \begin{cases} 0 \le \alpha_n \le C, \\ \sum_{n=1}^{N} \alpha_n y_n = 0, \end{cases} n = 1, \dots N$$

Here, the major consideration is the choice of the two parameters values C and σ. For the determination of optimal variables C and σ, classical models make use of trial-and-error approaches. It leads to high computational complexity and does not satisfy the way of finding the optimum or near optimum solution. PSO algorithm can be applied for the parameter optimization. PSO is a global optimization model stimulated from the motion of bird flocking or fish schooling. It is easier to design and offers quick implementation. PSO carried out a searching process through a group of particles updated from every round.

For seeking the optimum solutions, every particle shifts in the direction of its preceding best (p_{best}) and best global (g_{best}) positions in the swarm.

$$p_{best_m} = p_m(k^*) \quad (11)$$

$$st.fitness(p_m(k^*)) = \min_{k=1,\dots,t} [fitness(p_m(k))],$$

$$g_{best} = p_{m^*}(k^*) \quad (12)$$

$$s.t.fitness(p_m(k^*)) = \min_{\substack{m=1,\dots,p \\ k=1,\dots,t}} [[fitness(p_m(k))]$$

where m represents the particle index, P indicate the particle count, k is the round index, t represent the round number, and p indicates the position. The updation of the velocity and position of particles takes place using Eq. (13) and Eq. (14):

$$V_m(t+1) = wv_m(t) + c_1r_1\left(p_{best_m}(t) - p_m(t)\right) + c_2r_2\left(g_{best}(t) - p_m(t)\right) \quad (13)$$

$$p_m(t+1) = p_m(t) + V_m(t+1) \quad (14)$$

where V indicates the velocity. The inertia weight w employed for balancing the global exploration as well as local exploitation. The r_1 and r_2 undergo uniform distribution of the arbitrary parameters present in the range of $(0,\ 1)$. The $c_1$and c_2 are positive constant variables known as "acceleration coefficients." In this case, the encoding of particles contains the variables C and σ in (13). The process involved in the classification process is shown clearly in Fig. 4.

D. Cross-Validation

This paper applied the process of 5-fold cross validation assuming the optimal tradeoff among computation complexity and reliability estimation. The entire dataset undergo partition of 5 mutually exclusively subset of around equivalent sizes where a collection of 4 subsets are applied to train and final subset is employed to test the model. This process gets iterated over 5 times, therefore, every one subset is utilized for testing. The fitness function of PSO algorithm for choosing the classifier accuracy is given below.

$$fitness = \frac{1}{5}\sum_{i=1}^{5}\left|\frac{y_s}{y_s + y_m}\right| \quad (15)$$

Where y_s and y_m denotes the number of winning categorization and mis-classification, correspondingly. PSO is executed for the maximum of the fitness function (classifier performance).

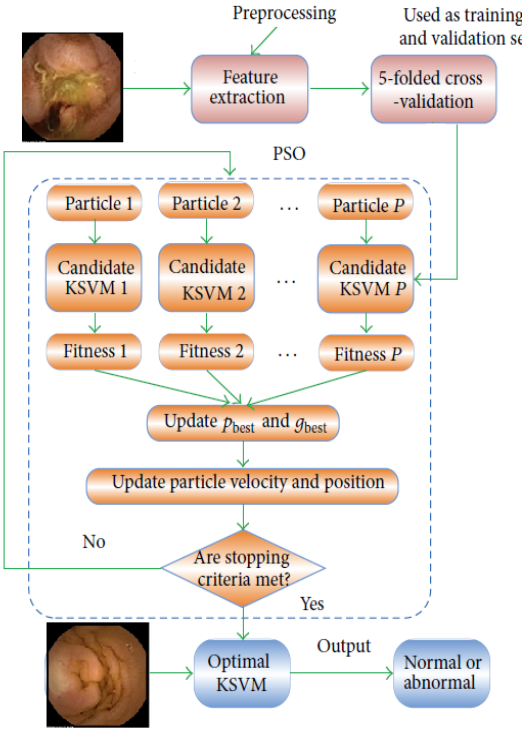

Fig. 4. Process involved in PSO-KSVM model

III. EXPERIMENTAL VALIDATION

A set of simulations takes place for measuring the efficiency of the presented model in an empirical way. A detailed experimental analysis takes place in the following subsections.

A. Dataset used

A set of almost 3500 WCE images are filtered from the collection of 16 bleeding and 16 non-bleeding videos captured from 32 patients [13]. The labels are provided to the images by trained physicians.

The equivalent frames are eliminated to prevent unwanted recurrence of images. The non-informative frames which are degraded using leftover food, turbid fluid, bubble, specular reflection or fecal content are not eliminated. It is carried out because of the fact that the implementation details should imitate real time environment. Under real-time applications, it is extremely improbable that a fresh collection of bleeding and non-bleeding images is accessible to the medical doctors. So, an efficient and practical technique has the capability to deal with the frames. Apart from the obviously repeated frames, every filtered frame from the set of 32 videos are utilized for the construction of the dataset. The training dataset holds a set of 600 bleeding as well as 600 non-bleeding frames captured from 12 diverse people. It is applied for training the SVM classification model. At the same time, the testing dataset holds a set of 860 bleeding as well as 860 non-bleeding frames gathered from the remaining set of patients. Fig. 5 shows the sample bleeding and non-bleeding cases. In addition, the respective magnitude spectrum is also clearly illustrated.

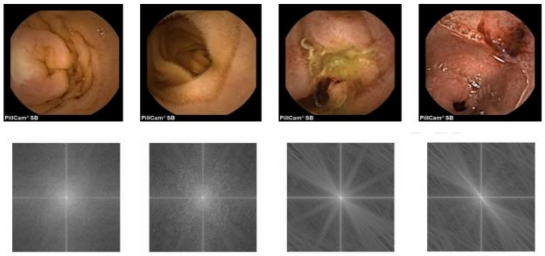

Fig. 5. Sample images with respective magnitude spectrums

A detailed experimental analysis takes place to validate the superior performance of these methods interms of accuracy, sensitivity and specificity. Table 1 tabulates the comparison of the results attained by diverse methods.

B. Results analysis

Fig. 6 illustrates the comparison of the experimental results attained by diverse models with respect to accuracy. The figure indicates that the existing RHR model exhibits inefficient classification over the other methods. It is confirmed by looking into the minimum accuracy value of 73.72%. Next to that, the PNN model portrays its poor classification performance over all the compared methods interms of accuracy except the RHR model. It is evident from seeing the slightly higher accuracy of 74.48%. At the same time, the CM-LBP model achieves moderate results by attaining somewhat better accuracy value of 77.74%. In line with, the SP model tries to attain competitive classification over the projected model by attaining a better accuracy value of 91.51. However, it does not have the ability to outperform the presented method. The maximum classification accuracy of 92.45 is achieved by the projected approach due to the inherent effective features and proper prediction on the applied test images.

Table- I: Results analysis of diverse models

Methods	Accuracy	Sensitivity	Specificity
SP	91.51	89.07	93.95
CM_LBP	77.74	76.28	79.19
PNN	74.48	75.93	73.02
RHR	73.72	75.35	72.09
Proposed	92.45	90.76	94.65

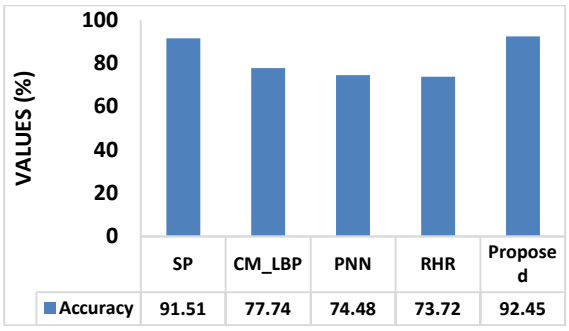

Fig. 6. Accuracy analysis of the presented model

Fig.7 demonstrates the comparative classifier performance attained by diverse models with respect to sensitivity. The figure indicates that the existing RHR model exhibits inefficient classification over the other methods. It is confirmed by looking into the minimum sensitivity value of 75.35%. Next to that, the PNN model portrays its poor classification performance over all the compared methods interms of sensitivity except the RHR model. It is evident from seeing the slightly higher sensitivity of 75.93%. At the same time, the CM-LBP model achieves moderate results by attaining somewhat better sensitivity value of 76.28%. In line with, the SP model tries to attain competitive classification over the projected model by attaining a better sensitivity value of 89.07. However, it does not have the ability to outperform the presented method. The maximum classification sensitivity of 90.76 is achieved by the projected approach due to the inherent effective features and proper prediction on the applied test images.

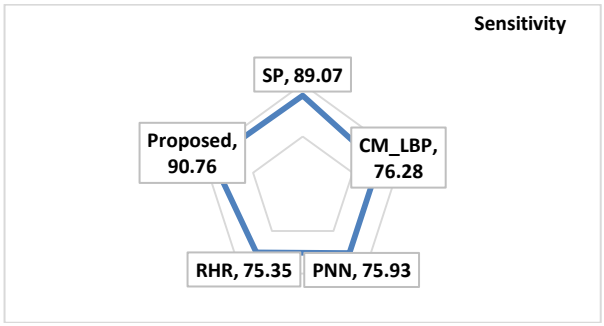

Fig. 7. Accuracy analysis of the presented model

Fig. 8 depicts the comparison of the experimental performance attained by diverse models with respect to specificity. The figure indicates that the existing RHR model exhibits inefficient classification over the other methods. It is confirmed by looking into the minimum specificity value of 72.09%. Next to that, the PNN model portrays its poor classification performance over all the compared methods interms of specificity except the RHR model. It is evident from seeing the slightly higher specificity of 73.02%. At the same time, the CM-LBP model achieves moderate results by attaining somewhat better specificity value of 79.19%. In line with, the SP model tries to attain competitive classification over the projected model by attaining a better specificity value of 93.95%. However, it does not have the ability to outperform the presented method. The maximum classification specificity of 94.65% is achieved by the projected approach due to the inherent effective features and proper prediction on the applied test images.

From the observance of the values present in the tables and figures, it can be easily verified that the projected model accurately classifies the applied GI images by attaining the highest accuracy of 92.45%, sensitivity of 90.76%, and specificity of 94.65%. In addition, the presented model is found to be an appropriate tool for the effective identification of disease.

IV. CONCLUSION

This paper has presented an efficient feature extraction-based classification model. An efficient NGLCM is applied for extracting the features of the GI images. The parameter tuning of SVM takes place using the PSO algorithm which will be helpful to classify theGI images into bleeding and non-bleeding regions.

Then, a KSVM-PSO algorithm is applied for the classification of the processed GI images. A set of simulations takes place for measuring the efficiency of the presented model in an empirical way. The results confirmed the enhanced classifier outcome of the presented model on all the applied images under several aspects. As a part of future scope, the presented model can be employed in real time scenarios..

REFERENCES

1. G. Iddan, G. Meron, A. Glukhovsky, P. Swain, Wireless capsule endoscopy, Nature 405 (2000) 417–417.
2. http://www.fda.gov/cdrh/mda/docs/k010312.html.
3. http://www.givenimaging.com.
4. Y. Fu, W. Zhang, M. Mandal, M.-H. Meng, Computer-aided bleeding detection in wce video, Biomedical and Health Informatics, IEEE Journal of 18 (2) (2014) 636–642.
5. R. Kumar, Q. Zhao, S. Seshamani, G. Mullin, G. Hager, T. Dassopoulos, Assessment of crohn's disease lesions in wireless capsule endoscopy images, Biomedical Engineering, IEEE Transactions on 59 (2) (2012), 355-362.
6. B. Li, M.-H. Meng, Computer-aided detection of bleeding regions for capsule endoscopy images, Biomedical Engineering, IEEE Transactions on 56 (4) (2009) 1032-1039.
7. S. Hwang, J. Oh, J. Cox, S. J. Tang, H. F. Tibbals, Blood detection in wireless capsule endoscopy using expectation maximization clustering, in: Proc. SPIE, Vol. 6144, 2006, pp. 1–11.
8. R. Kumar, Q. Zhao, S. Seshamani, G. Mullin, G. Hager, T. Dassopoulos, Assessment of crohn's disease lesions in wireless capsule endoscopy images, Biomedical Engineering, IEEE Transactions on 59 (2) (2012), 355-362.
9. G. Pan, G. Yan, X. Qiu, J. Cui, Bleeding detection in wireless capsule endoscopy based on probabilistic neural network, Journal of Medical Systems 35 (6) (2011) 1477–1484
10. J. Liu, X. Yuan, Obscure bleeding detection in endoscopy images using support vector machines, Optimization and Engineering 10 (2) (2009) 289–299
11. Scale invariant texture descriptors for classifying celiac disease, Medical Image Analysis 17 (4) (2013) 458 – 474.
12. J. Cunha, M. Coimbra, P. Campos, J. M. Soares, Automated topographic segmentation and transit time estimation in endoscopic capsule exams, Medical Imaging, IEEE Transactions on 27 (1) (2008) 19–27
13. http://www.cse.oulu.fi/cmv/downloads/lbpmatlab.

AUTHORS PROFILE

R Ponnusamy received B.Sc degree in Computer Science from Bharathidhasan University, M.C.A degree from Madurai Kamarajar University and M.Phil degree from Annamalai University, India. He joined the Department of Computer Science and Engineering, Annamalai University in the year 2002. At present he is working in the Department of Computer and Information Science, Annamalai University. He has almost 18 years of teaching experience. He is currently pursuing Ph.D degree in the Department of Computer and Information Science, Annamalai University. His research interests include Medical image analysis, Data mining and Content-based image retrieval.

S.Sathiamoorthy received B.Sc degree in Physics from University of Madras, M.C.A degree from Bharathidasan University and M.Phil as well as Ph.D. from Annamalai University, India. In the year 2001, he joined in the Department of Computer Science and Engineering, Annamalai University and also served in the Computer Science and Engineering Wing of Directorate of Distance Education and Department of Computer and Information Science, Annamalai University. At present, he is Assistant Director (Controller of Examinations), Tamil Virtual Academy, Information Technology Department of Tamil Nadu Government, India. He has almost 19 years of teaching experience. Currently he is working on Pattern recognition, Pattern analysis, Image retrieval and classification. His research interests include Machine learning algorithms and Medical image analysis. He has published more than 25 papers in various International journals and more than 15 papers in national and international conferences. He has been on the reviewing and editorial board of many reputed journals.